

## Multiple-step recrystallization within massive ancient dolomite units: an example from the Dinantian of Belgium

P. NIELSEN,\* R. SWENNEN† and E. KEPPENS\*

\*Geochronology, V.U. Brussels, Pleinlaan 2, B-1050 Brussels, Belgium

†Fysico-chemische Geologie, K.U. Leuven, Celestijnenlaan 200C, B-3001 Heverlee, Belgium

### ABSTRACT

South of the Caledonian Brabant – Wales Massif a more than 200 m thick Tournaisian to Lower Visean replacive dolomite unit can be followed for several hundred kilometres from the Boulonnais (France) to Aachen (Germany). Field observations, of features such as karst cavities occurring at the top of the Lower Visean dolomite which are filled by Lower Visean crinoidal limestone, indicate that dolomitization and karstification took place during the Early Visean. This early development of the dolomite is in agreement with the presence of stylolites cutting the dolomite fabric. The minor element composition of the majority of the dolomites remains almost uniform throughout the entire studied area. Values for Fe, Mn, Na and Sr are normally in the range 700–4700 ppm, 15–400 ppm, 80–300 ppm and 50–200 ppm, respectively. The  $\delta^{13}\text{C}$  values (range –0.72 to +5.31‰) mainly reflect the carbon isotopic composition of the precursor limestones. The  $\delta^{18}\text{O}$  values, in contrast, are highly variable: ranging from –19.15 to +0.85‰. This rather large range of  $\delta^{18}\text{O}$  values is explained by multiple-step re-equilibration/recrystallization during progressive burial and subsequent uplift of the dolomites. These processes are also responsible for the high  $^{87}\text{Sr}/^{86}\text{Sr}$  values of the dolomites which range from about 0.7088 to 0.7098. They are distinctly more radiogenic than Lower Visean marine carbonates (0.7076–0.7078). Correlation, however, of  $\delta^{18}\text{O}$  values or  $^{87}\text{Sr}/^{86}\text{Sr}$  ratios with dolomite and/or cathodoluminescence (CL) textures has not been very successful. This suggests that recrystallization may remain unrecognized if only petrographic techniques are used. Nevertheless, certain CL textures can be related to specific interactions with the ambient recrystallizing fluids.

### INTRODUCTION

According to Land (1985), Given & Wilkinson (1987) and many others, seawater is the prime common fluid that provides enough Mg for pervasive dolomitization. Therefore, most of the massive dolomites which formed within the shallow burial realm are thought to be derived from seawater related fluids. Geochemical data of ancient dolomites, however, are often not compatible with such an origin (Land, 1980, 1985; Banner *et al.*, 1988; Cander *et al.*, 1988; Gao, 1990; Gao & Land, 1990). This discrepancy is often considered to be the result of one or more recrystallization events during which metastable dolomites are converted to more stable dolomite. Whether this occurs by a single continuous process or involves step-wise dissolution – reprecipitation events is still debated (Sperber *et al.*, 1984; Land, 1985;

Sibley, 1990). Since recrystallization may take place in settings different from those of initial dolomite formation, important geochemical and textural modifications may occur. Therefore, some authors (e.g. Montañez & Read, 1992a) recently pointed out that the origin of ancient dolomites could be delineated, despite dolomite modification, by evaluating the general geological setting.

The Lower Dinantian succession south and south-east of the Caledonian Brabant – Wales Massif (Belgium) mainly consists of dolomitized, shallow marine carbonates (Fig. 1). Field and petrographic data gathered from the area between Namur – Hoyoux and Aachen indicate that dolomitization occurred within the shallow burial realm (Swennen *et al.*, 1988). Dolomitization by reflux of (hyper)saline

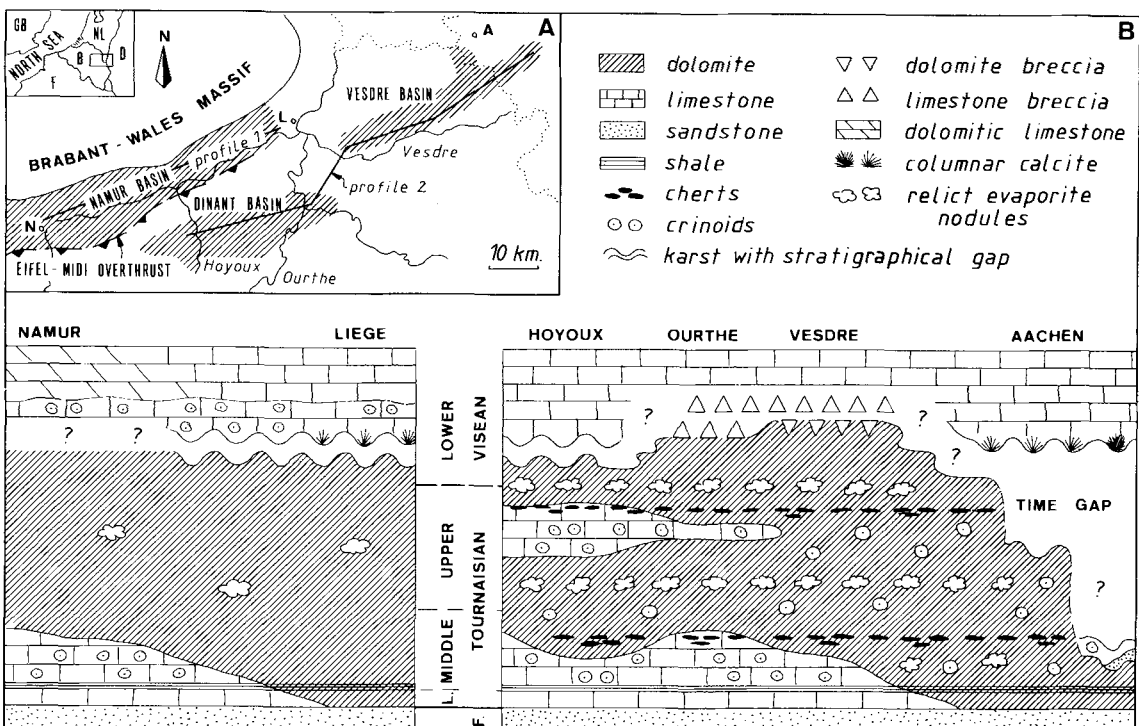


**Fig. 1.** (A) Location map of the study area, with areal distribution of the Lower Dinantian dolomites (N, Namur; L, Liège; A, Aachen). (B) Schematic cross-section through the study area giving the stratigraphical framework during the Lower Dinantian. Thickness is not to scale. (L, Lower; F, Famenian.)

brines and/or dolomitization due to seawater circulation near the mixing zone during a sea level lowstand are likely models to explain their formation. The Lower Dinantian dolomites are, however, depleted in  $^{18}\text{O}$  and they possess low Na and Sr contents and relatively low Fe and Mn contents.

This paper addresses the multiple-step recrystallization that followed initial dolomite precipitation. The study indicates that dolomite crystals within one locality, and even within one sample, can remain nearly unaltered while others are extensively modified. To deduce the origin and timing of dolomitization, special attention will first be paid to the geological context.

## GEOLOGICAL SETTING

Lower Dinantian replacive dolomites crop out along the southern to south-eastern margin of the Brabant-Wales Massif (Fig. 1A) from the Boulonnais (near Calais, France) to Aachen

(Germany). In the studied area these dolomites occur within the autochthonous Namur Basin, as well as in the allochthonous Dinant and Vesdre basins. Tectonic displacement along the Eifel-Midi overthrust is believed to be in the order of several tens of kilometres (Bless *et al.*, 1980). This displacement reflects the important regional pre-Variscan distribution of these dolomites. Dolomites also occur in the subsurface of the Campine basin, north of the Brabant-Wales Massif.

South of the Brabant-Wales Massif shallow marine Tournaisian to lowermost Visean limestones have been dolomitized (Fig. 1B; Paproth *et al.*, 1983a). The dolomites are most massively developed in the Vesdre area. Based on composite sections the total thickness can be estimated to be at least 200 m. In the Ourthe and Hoyoux areas the dolomites interfinger with pure massive bedded crinoidal packstones to grainstones or organic/clay-rich mudstones. The contact between dolomite and limestone here is diachronous (Fig. 1B). In the Aachen and Namur-Liège areas it is impossible to infer the original

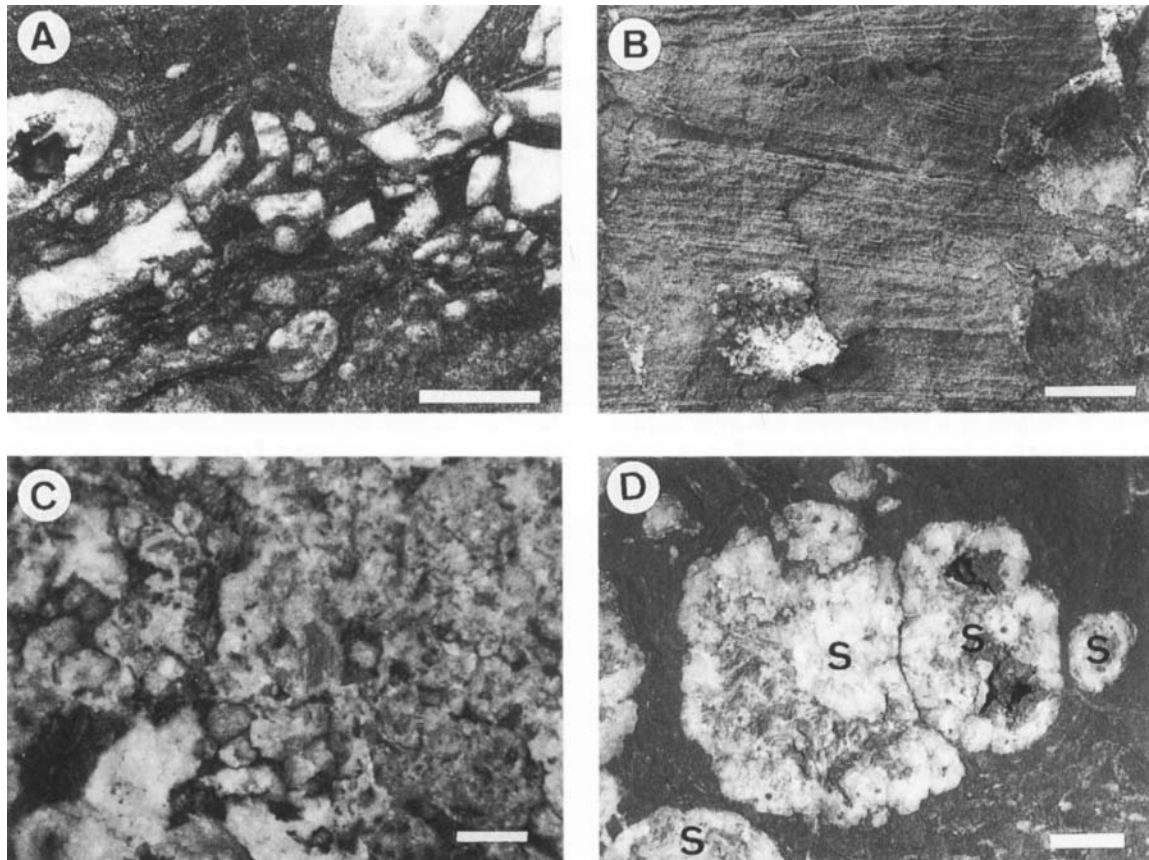


**Fig. 2.** (A) Macroscopic view of crinoidal dolomite which mainly occurs at the base of the dolomite succession. Scale bar=2 cm. (B) Macroscopic view of weathered dolomite surfaces displaying cross bedding. Scale bar=2 cm. (C) Macroscopic view of pseudomorphosed evaporites displaying a chickenwire structure. Scale bar=1 cm. (D) Macroscopic view of silicified anhydrite nodules (S) exhibiting a cauliflower outline. Scale bar=2 cm.

thickness of the dolomites since the top of the dolomites is intensively karstified in both areas. Locally, karst cavities may reach down to about 15 m.

Despite the fact that dolomitization obliterated most of the sedimentary structures, it can be inferred from non-dolomitized limestone intercalations and from cherts occurring within the dolomites that mainly shallow marine subtidal carbonates are dolomitized (Boonen & Kasig, 1979; Kasig, 1980; Swennen, 1986). Within the upper 80 m of the massive dolomites in the Vesdre – Ourthe area (Fig. 1A, B) a gradual shallowing upward trend is evident. Initially, crinoidal dolomites predominate (Fig. 2A), but they pass upward into parallel and cross bedded dolomite (Fig. 2B) with decreasing crinoid content.

They finally pass into cyclical sediments in which organic-rich finely crystalline dolomites dominate. In the uppermost strata some rare 1–5 cm thick coal intercalations occur, as well as sabkha units with cavernous dolomite, dolomitized microbial laminites and pseudomorphosed evaporites with chickenwire structure (Fig. 2C; Peeters *et al.*, 1992a). Locally symmetrical ripple marks have been recognized in this interval. Furthermore, two major chert horizons occur within the massive dolomites. Quartz and dolomite nodules, which commonly possess a cauliflower outline (Fig. 2D), are very common. These nodules, which were interpreted as pseudomorphs after anhydrite nodules (Swennen & Viaene, 1986), occur in subtidal sediments.

## TIMING AND MODELS OF DOLOMITIZATION

In the Vesdre – Ourthe area, the uppermost dolomites, which are interpreted as shelf interior deposits (Swennen, 1986), are overlain by up to 40 m thick evaporite dissolution collapse breccias (Swennen *et al.*, 1990; Vogel *et al.*, 1991; Peeters *et al.*, 1992a). Based on foraminiferal assemblages occurring in cherts, the uppermost dolomites yield an Early Visean age (Swennen, 1986). The breccias, which are not datable, are overlain by Lower Visean peritidal limestones (Paproth *et al.*, 1983a).

In the Aachen area the top of the massive dolomites is marked by a karst horizon and karst cavities are filled with columnar calcites (Fig. 1B). Karstification in this area may explain the variation in dolomite thickness, which is normally between 100 and 150 m, but locally is reduced to about 15 m. The dolomitized limestones have tentatively been dated as Middle to Late Tournaisian (Kasig, 1980). They are overlain by Lower Visean crinoidal and oolitic limestones (Paproth *et al.*, 1983a).

Closest to the Brabant – Wales Massif (Namur – Liège area) the top of the dolomites is also marked by a karst horizon (Pirlet, 1970). On the basis of relic coral assemblages (Viel, 1984), the dolomitized limestones are of Early Visean age. The karst cavities are mainly filled by columnar calcite (Swennen *et al.*, 1981). Within some of the cavities, however, geopetally organized, non-dolomitized crinoidal sediments occur. The latter are identical in composition to the overlying Lower Visean non-dolomitized crinoidal limestones. Consequently, karstification and dolomitization pre-date deposition of the crinoidal sediments and are both Early Visean in age.

The lower dolomite/limestone contact is diachronous. In the Vesdre and Namur – Liège area the lowermost dolomites occur in contact or just above a 20 m thick basal Middle Tournaisian shale unit (Fig. 1B). In the Aachen area the massive dolomites crosscut these shales (Fig. 1B).

As illustrated above, the major period of dolomitization is of Early Visean age and is topped by a karst which reflects lowering of sea level. Whether this corresponds to the 347 Ma sea level lowstand described by Ross & Ross (1987) is unclear, although late diagenetic dolomitization models can consequently be excluded. This is also in agreement with the fact that the dolomites locally are crosscut by stylolites and fractures. The most likely dolomitization mechanisms are evaporative seawater reflux

and/or dolomitization due to seawater circulation near the mixing zone. The latter cannot be excluded since an important karst horizon marks the upper dolomite contact in areas near the Brabant – Wales Massif (Muchez, 1988; Peeters *et al.*, 1992b). This model is also compatible with an early development and the gradual shallowing upward trend within the upper dolomites. Seawater involvement could also explain the development of diagenetic anhydrite nodules. A more viable mechanism to explain the occurrence of these nodules within normal saline subtidal dolomitized strata, however, is evaporative reflux dolomitization (Maliva, 1987). Furthermore, the fact that the dolomites are best developed where they are capped by evaporitic dissolution collapse breccias favours this model. Dolomitization by dense evaporative brines is also more likely, taking into account the vast amount of dolomite ( $>10^{12} \text{ m}^3$ ) formed in a relatively short period of time (Harland *et al.*, 1989).

## METHODS

More than 200 thin-sections from 10 profiles have been studied with conventional, cathodoluminescence (CL) and fluorescence petrography. CL petrography was carried out with Technosyn Cold Cathodo Luminescence Model 8200 Mark II. Operating conditions were 16–20 kV gun potential, 420  $\mu\text{A}$  beam current, 0.05 Torr vacuum and 5 mm beam width.

Incident light fluorescence microscopy was carried out with a Nikon Labophot using an Hg lamp, an excitor filter (Nikon 515 W) and a diachromatic beam splitter (see also Dravis & Yurewicz, 1985). More than 20 samples have been studied in detail by backscatter electron microscopy (Jeol JSM-6400-BSE).

Dolomite stoichiometry was determined by X-ray diffraction analyses of whole rock samples. The proportion of calcium in the dolomite was determined by measuring the dolomite (104) peak shift with respect to an internal quartz standard. The  $\text{CaCO}_3$  content was then calculated using Lumsden's (1979) equation [ $\text{mol\% CaCO}_3 = 333.33 \times d(104) - 911.99$ ], where  $d$  is the observed  $d$ -spacing ( $\text{\AA}$ ).

Ca, Mg, Sr, Na, Fe and Mn concentrations were obtained by atomic absorption spectrometry (AAS). Carbonate powder of 0.5 or 0.1 g was dissolved in concentrated HCl. The analytical procedure has been described by Swennen *et al.* (1986). Analytical precision at the 95% confidence level determined on

**Table 1.** Lower Dinantian dolomite types of Belgium classified according to Sibley & Gregg (1987).

Type	Texture	Crystal size	CL characteristics	Fluorescence characteristics
Relic crystals	planar-e	20–50 µm	Intracrystalline	
1A	planar-s	20–60 µm	non to dull brown/red	mottled to patchy
1B	non-planar to planar-s	80–250 µm	non to dull brown/red	mottled to patchy
1C	planar-e	50–250 µm	non to dull brown/red	mottled to patchy
2A	non-planar to planar-s	0·1–10 mm	dull reddish	homogeneous
2B	non-planar to planar-s planar-e	200–750 µm 1–3 mm	dull to bright red non/dull red zoned	patchy patchy
3	planar	20–500 µm	dull to bright, often zoned	homogeneous

replicate analyses is better than 10%. However, it was not always possible to sample large enough quantities of certain dolomite types to carry out AAS analysis. This also hindered isotopic analyses of one of the dolomite types described below.

After careful petrographic characterization of individual authigenic minerals, a microscope mounted micro-drill assembly (with a drill-bit of 0·5–1 mm) was used to obtain carbonate powders of 1–10 mg for isotopic analysis. Isotopic analysis of carbon and oxygen was performed on a Finnigan Mat delta E stable isotope ratio mass spectrometer. Carbonate powders were dissolved in  $\pm 100\%$  orthophosphoric acid at 25°C. All data have been corrected following procedures modified from Craig (1957). The isotopic compositions are expressed as  $\delta$  values in per mil ( $\text{‰}$ ) difference from the PDB international standard. Reproducibility, determined by replicate analysis of NBS 19 and NBS 20, is better than 1·0‰ for oxygen and 0·05‰ for carbon. No correction for dolomite dissolution by phosphoric acid has been applied, following the recommendation of Land (1980).

Sr isotope analyses were performed on a Finnigan Mat 260 or a VG Sector 54 mass spectrometer. Carbonate powders of about 10 mg were dissolved in concentrated HCl. Sr was separated using standard cation exchange techniques. Replicate analyses of the NBS 987 strontium standard yielded an average  $^{87}\text{Sr}/^{86}\text{Sr}$  ratio of 0·710211, with a standard deviation ( $\sigma$ ) of  $\pm 0\cdot000006$ . All  $^{87}\text{Sr}/^{86}\text{Sr}$  ratios were normalized to an NBS 987 value of 0·710140 in order to allow direct comparison with other data sets (cf. Popp *et al.*, 1986; Banner *et al.*, 1988; Smith & Dorobek, in press).

## PETROGRAPHY

The most important dolomite types are given in Table 1. Early dolomites are differentiated from late dolomites. The former are replacive in origin and make up the bulk (>90%) of the studied sequence, whilst the latter consist of saddle dolomites and dolomite cements.

### Early dolomite

#### *Transmitted light microscopy*

The early pervasively dolomitized rocks generally consist of planar-s to non-planar dolomite fabrics (Sibley & Gregg, 1987). Dolomite texture and crystal size distribution are mainly influenced by the precursor lithology. Within organic/clay-rich lithologies, dark, dense finely crystalline (20–60 µm) dolomites (type 1A) are present. In the more pure dolomites (HCl insoluble residue <3%) medium to coarsely crystalline (80–250 µm) dolomites predominate (type 1B). In both populations uni- and bimodal distributions can be differentiated. The coarser crystalline dolomites may possess vuggy, biomouldic and/or intercrystalline porosities of up to 10%. The dolomite crystals are commonly cloudy to clear throughout; some, however, have a cloudy centre and clear rim.

Pre-existing dolomites have been rarely observed. They occur as small euhedral ghost or relic crystals (20–50 µm) within the centre of some type 1 dolomite crystals (see Fig. 4A). Similar euhedral crystal relics were also found in chert nodules (Swennen, 1986).

At the dolomitization front, dispersed 50–250 µm euhedral dolomite crystals occur (type 1C; planar-e to planar-s fabric of Sibley & Gregg, 1987). Here also

the precursor lithology seems to exert a major control on crystal size. Within micritic limestone relatively small crystals ( $\pm 50 \mu\text{m}$ ) dominate and within packstones and grainstones relatively large dolomite crystals (100–250  $\mu\text{m}$ ) are present. Most of the larger crystals have a cloudy centre and clear rim. Crystal sizes vary most at the dolomitization front, where a large range of crystal sizes within a single sample are present.

According to Gregg & Sibley (1984), dolomite crystal growth at temperatures below 50°C should produce mostly planar textures. Above the so-called 'critical roughening temperature' (CRT), non-planar textures would develop more frequently. Since planar and non-planar dolomite textures occur in the studied sequence, application of the dolomite crystal growth theory is not straightforward. It cannot be excluded that the non-planar textures originate from neomorphism of pre-existing dolomites at temperatures exceeding the CRT. However, theoretically, non-planar dolomite textures can also develop below the CRT at high supersaturation levels.

Although the relic crystals within some type 1 dolomite crystals could be interpreted as relic crystals of pre-neomorphosed dolomite, since chertification pre-dates type 1 dolomite formation, it is more likely that the relic crystals which also occur in the cherts reflect a first dolomite generation. Since their total contribution is minor (<0.1%) they will not be further discussed.

#### *Cathodoluminescence microscopy (CL) and backscatter electron microscopy (BSE)*

The early dolomites are generally characterized by an absence of visible luminescence or by a dull brown/

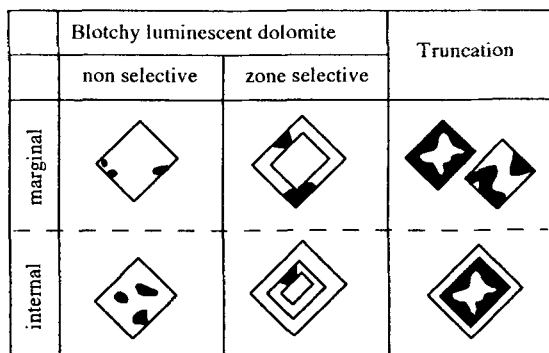


Fig. 3. Textures visible with cathodoluminescence interpreted as due to recrystallization.

red luminescence. In detail the following luminescence textures can be differentiated (Fig. 3).

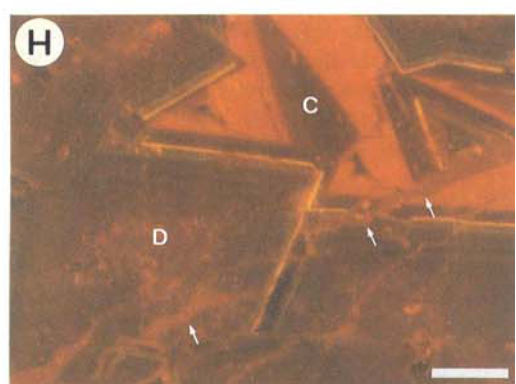
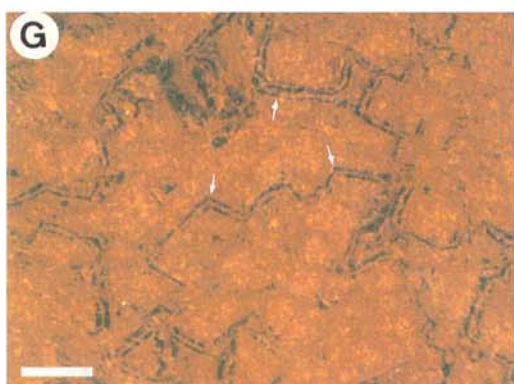
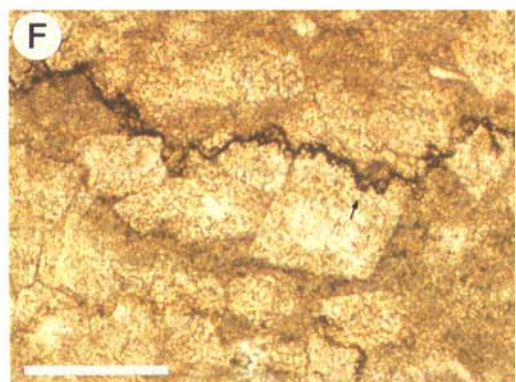
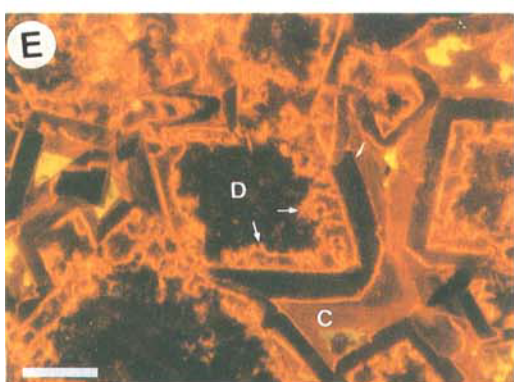
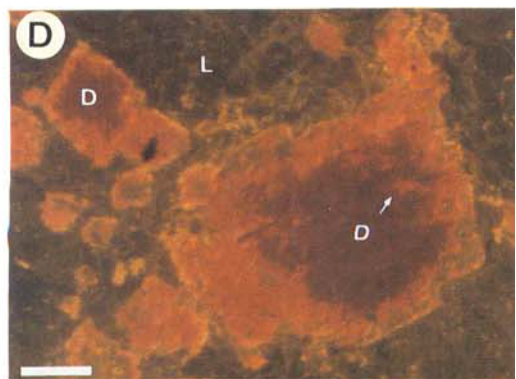
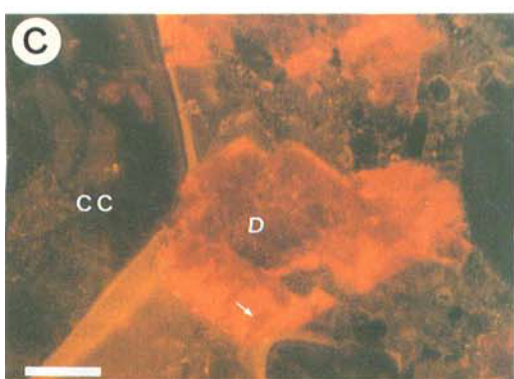
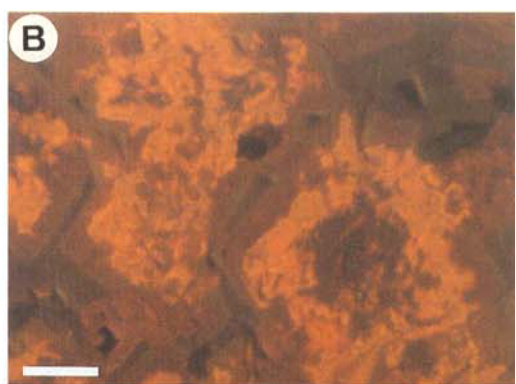
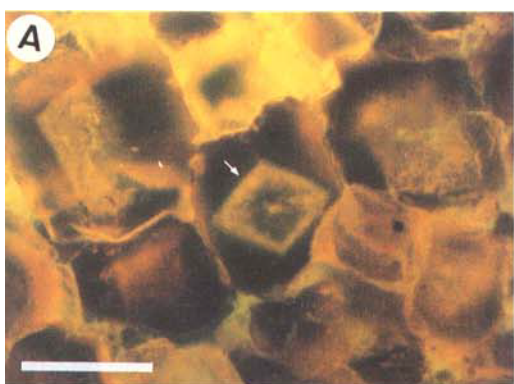
**1** Dolomite displaying homogeneous to semi-homogeneous luminescence.

**2** Non- to dull luminescent dolomite with interspersed patches of a brighter luminescent dolomite generation (Fig. 4B). The size of these patches varies from a few to several tens of micrometres, replacing large parts of the original dolomite crystals. Locally these patches are restricted to certain zones of the dolomite crystals. This texture with interspersed patches clearly is not primary.

**3** Irregular (truncation) contacts within dolomite crystals (Fig. 4C–E).

No compositional differences within the type 1 dolomite crystals of these samples were detected using BSE textural analysis. Some crystals, however, contained abundant calcite 'spots'. These calcite 'spots' can be interpreted as relics of a precursor limestone

**Fig. 4.** (A) Fluorescence photomicrograph of anhedral type 1 dolomite crystals with ghosts of small individual euhedral crystals present within the centre. Scale bar = 20  $\mu\text{m}$ . (B) Cathodoluminescence (CL) photomicrograph of type 1 dolomite with a blotchy luminescence appearance. The randomly interspersed dull yellow-orange luminescent patches are interpreted as recrystallized dolomite. Scale bar = 50  $\mu\text{m}$ . (C) CL photomicrograph of a single planar dolomite crystal (D) bordered by non-bright to dull luminescent calcite cement (CC) that pre-dates dolomitization. This crystal is composed of an outer dull to bright red luminescent part and an inner darker part. The contact between both is irregular and within the dull to bright part patches of the darker generation are present. Scale bar = 50  $\mu\text{m}$ . (D) CL photomicrograph of type 1 dolomite crystals (D) consisting of two dolomite generations. The contact between both is irregular (arrow). Although the crystals are of different size they display the same characteristics. (L, micritic limestone.) Scale bar = 100  $\mu\text{m}$ . (E) CL photomicrograph of type 1 dolomite crystals (D) with an internal truncation surface (arrows). Intercrystalline porosity is filled by dolomite cement (C) and patches of yellow luminescent calcite cement. Scale bar = 50  $\mu\text{m}$ . (F) Microphotograph of type 1 dolomite rhombs affected by stylolitization (arrow) indicating that the latter post-dates type 1 dolomitization. Scale bar = 100  $\mu\text{m}$ . (G) CL photomicrograph displaying relics/ghosts of zoned CL patterns most likely after type 3 dolomite cements. This testifies to homogenization by late recrystallization. Scale bar = 100  $\mu\text{m}$ . (H) CL photomicrograph of type 1 dolomite (D) and type 3 dolomite cement (C). Locally, microfractures crosscut both dolomite types. These microfractures can affect large parts of the surrounding dolomite (arrows). Scale bar = 50  $\mu\text{m}$ .



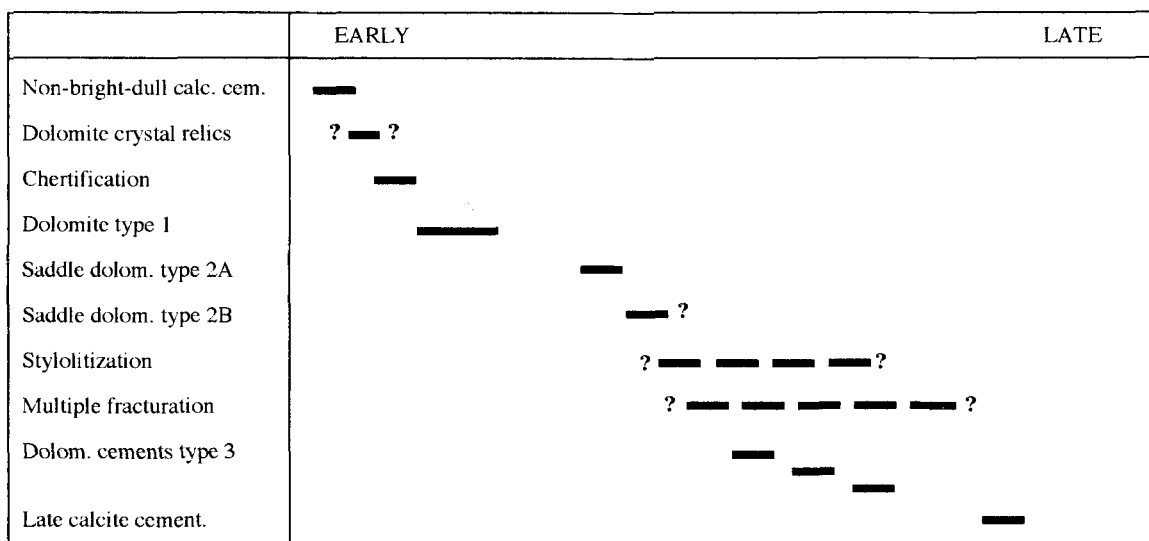


**Fig. 5.** Schematic sequence of the most important carbonate minerals occurring within the Lower Dinantian dolomites of the study area.

or they may have formed due to exsolution of a calcian-rich dolomite during recrystallization towards more stoichiometric dolomite.

### Late dolomite

#### Transmitted light microscopy

Dolomite type 2 consists of saddle dolomites. Different subtypes are recognized. Non-planar, coarsely crystalline, void filling saddle dolomite (type 2A) commonly occurs in dissolved sulphate nodules and crinoid moulds. In the eastern part of the study area, replacive and void filling, non-planar and planar-e saddle dolomites (type 2B) occur in association with Mississippi Valley-type mineralizations (MVT) (Swennen, 1986).

Dolomite type 3 consists of several dolomite cement generations that have been grouped together. They mainly occur as void fills and fracture fills and are nearly inclusion-free. Within the thin (commonly less than 1 mm thick) fractures and voids, this dolomite type forms euhedral overgrowths (tens to several hundreds of micrometres thick) on the early type 1 dolomites.

#### Cathodoluminescence microscopy

The type 2A saddle dolomites generally display a dull reddish luminescence. The type 2B cements occur

either as dull to bright red luminescent non-planar crystal mosaics or as dispersed zoned euhedral crystals. Semi-homogeneous luminescent textures or textures with interspersed patches are also observed in both saddle dolomite types.

The type 3 dolomite cements commonly display a complex CL zonation pattern. An irregular surface usually characterizes the contact between type 1 and 3 dolomite. This surface probably testifies to a period of dissolution between both dolomite generations; overgrowth on non-planar crystal faces or fractured crystals are other possibilities.

### Paragenetic succession

A paragenetic succession of the important authigenic minerals has been determined, based on petrographic and CL observations of the studied dolomites (Fig. 5).

As deduced from field evidence, the main dolomitization period (type 1 dolomites) took place during the Early Visean. Its formation prior to chemical compaction is suggested by the fact that stylolites cut through the dolomite fabrics (Fig. 4F). Relics of dolomite minerals, developed before this pervasive dolomitization stage, are still present. Chertification pre-dates dolomite type 1 formation since the original limestone fabric is well preserved within several chert nodules (Swennen, 1986). At

**Table 2.** Range of trace element contents for 95% of the dolomite population in the different localities (number of analysed samples for each locality >30, unless otherwise indicated) and data reported by <sup>1</sup>Swennen (1986) and <sup>2</sup>Swennen & Viaene (1990).

Area	Sr (ppm)	Na (ppm)	Fe (ppm)	Mn (ppm)
Type 1: Liège <sup>1</sup>	78–123	75–154	403–2307	197–401
Type 1: Hoyoux ( <i>n</i> =15)	63–113	75–243	343–1243	36–133
Type 1: Aachen	32–85	83–216	705–4604	143–1245
Type 1: Ourthe <sup>1</sup>	50–145	70–227	338–1480	35–166
Type 1: Vesdre <sup>1</sup>	62–200	110–253	707–3548	67–109
Type 2A dolomite ( <i>n</i> =16)	157–302	49–97	68–189	44–133
Type 2B dolomite <sup>2</sup>	20–26	165–249	9160–13 308	1713–2383

the dolomitization front the type 1C dolomites post-date a non-bright to dull luminescent calcite cement, which mainly developed as a syntaxial overgrowth on crinoid fragments. Styolitization not only post-dates type 1 but also type 2A and 2B saddle dolomite formation since the latter are also locally crosscut by pressure dissolution seams. Fractures with different type 3 dolomite cements show crosscutting relationships indicating different episodes of fracturing and cementation. Since these strata were affected by the Variscan orogeny, the development of many of these fractures and cements within this time period is likely, although detailed evidence is lacking. During this period, these dolomites were at a depth of at least 3000 m (Oncken, 1984). Some of the fractures crosscut stylolites. Some of the dolomite cements also locally occur along stylolites, which suggests that the latter have acted as fluid conduits.

All the dolomite generations pre-date a late diagenetic, blocky calcite cement. This cement is characterized by alternations of bright yellow and non-luminescent zones. It can be seen to replace type 1 dolomites and certain zones within the MVT-related type 2B saddle dolomites. Normally, the volumetric importance of this calcite generation is very limited.

## GEOCHEMISTRY

Data reported in this part are mainly from five key profiles in which a large set of major, trace element and stable isotope data are available. However, data from other localities are in general agreement with those given below.

### Major and trace element composition

Most of the type 1 dolomites have a nearly stoichiometric composition with  $\text{CaCO}_3$  contents varying around  $50.0 \pm 0.8$  mol%.

As shown in Table 2, the overall Sr, Na, Fe and Mn composition of these relatively pure type 1 dolomites (HCl insoluble residue for 95% of the dolomites is less than 3%) remains almost uniform over the entire studied area. Sr values are typically around 80 ppm and Na values normally do not exceed 250 ppm. Fe and Mn values are also rather low: below 4000 ppm and below 200 ppm, respectively. Some of the Fe and Mn may originate from Fe–Mn oxides/hydroxides which occur mainly as intercrystalline generations and which are dissolved during HCl treatment (Swennen & Viaene, 1990).

The dolomites immediately below the evaporite dissolution collapse breccias have slightly higher Sr and Na contents. The lowest Sr and Na contents occur systematically near the dolomitization front (Swennen, 1986). No other apparent relationships have been recognized between the geochemistry and the stratigraphy, sedimentology or position within the dolomite body. The uniform trace element pattern reflects either that the type 1 dolomites were derived from a homogeneous fluid or that initial differences were erased by successive recrystallization events.

Type 2A saddle dolomites possess very low trace element contents; the low Fe content (57–189 ppm) is conspicuous. Type 2B MVT-related saddle dolomites, in contrast, are rich in Fe (9160–13 308 ppm) and also in Mn (1713–2383 ppm). Possibly the higher Fe and Mn values of the host

**Table 3.** Isotopic signature (‰) of the different dolomite types.

Dolomite type	No. of samples	$\delta^{13}\text{C}$ range	$\delta^{18}\text{O}$ range
1A	>10	+0.70 to +3.26	-15.78 to +0.85
1B	>100	-0.72 to +5.31	-19.15 to -100
1C	>40	+1.84 to +4.67	-14.40 to -1.60
2A	30	-1.35 to +2.84	-20.54 to -9.09
2B	4	-0.01 to +0.50	-6.90 to -6.16
3	5	-1.74 to +1.53	-11.00 to -9.87

dolomites (type 1) in the Aachen area (Table 2) are related to interference with these MVT-related fluids.

Type 3 dolomite cements could not be sampled in sufficient quantities for AAS analysis. However, they do not stain with potassium ferricyanide, indicating a relatively low Fe content.

#### Carbon and oxygen stable isotopes

The  $\delta^{13}\text{C}$  values for type 1 dolomites range from -0.72 to  $\pm 5.31\text{\textperthousand}$  (Table 3) and are well within the range of reported Lower Carboniferous marine carbonates (Fig. 6A). Contribution from other  $\text{CO}_2$  sources therefore seems generally of minor importance.

The  $\delta^{18}\text{O}$  compositions of these dolomites cover a range from +0.85 to -19.15‰ (Table 3, Fig. 6A).  $\delta^{18}\text{O}$  values of individual localities commonly cover the complete range (Fig. 6A). No consistent relation between  $\delta^{18}\text{O}$  and either dolomite fabric or CL

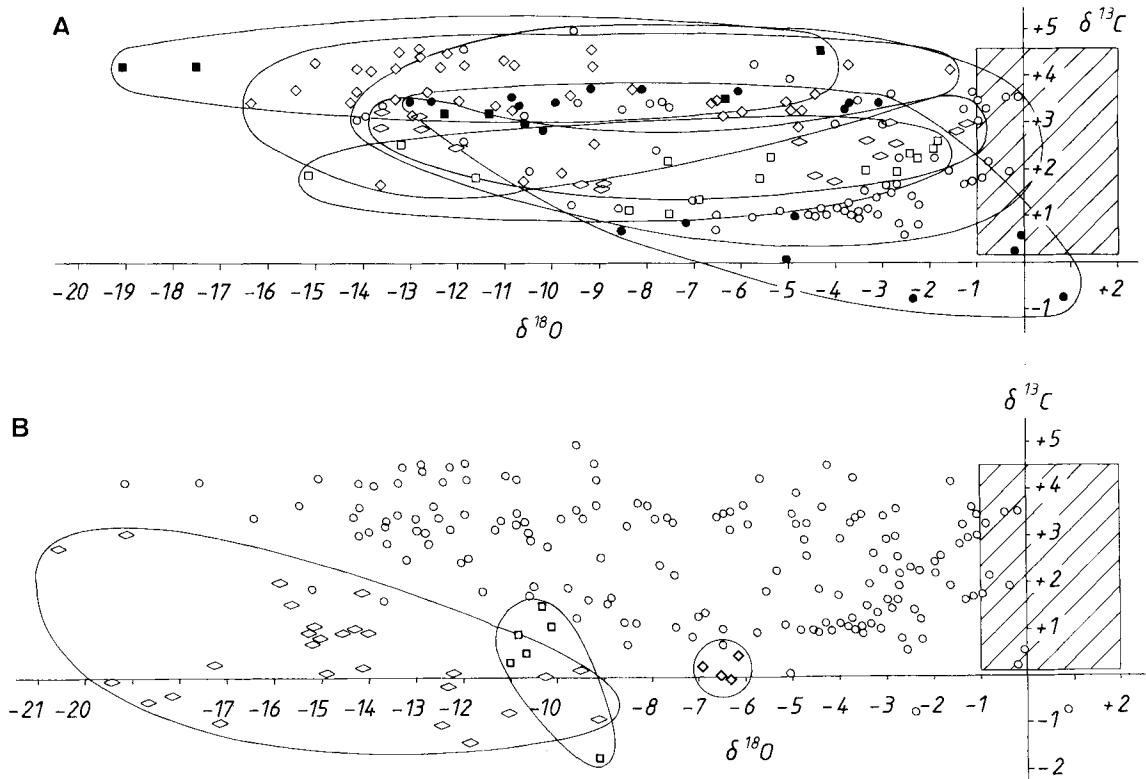


**Fig. 6.** Stable isotope plot of type 1 dolomites. Not all the studied profiles are shown. (■) Rivage (Ourthe), (◇) Belle Roche (Ourthe), (○) Saint Roch (Vesdre), (●) Walhorn (Vesdre), (◇) Modave (Hoyoux), (□) Binsfeldhammer (Aachen). (▨) Reference value for Lower Carboniferous marine dolomites (Brand, 1982; Meyers & Lohmann, 1985; Lohmann, 1987; Hudson & Anderson, 1989; Walkden & Williams, 1991). (B) Stable isotope plot of the different dolomite types. (○) Type 1 dolomites, (◇) type 2A saddle dolomites, (◇) type 2B saddle dolomites, (□) type 3 dolomite cements.

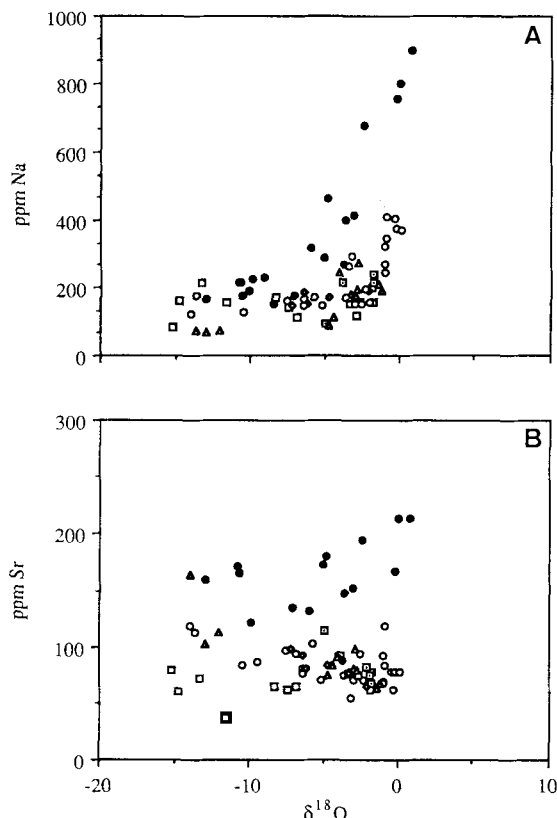


**Fig. 7.** (A)  $\delta^{18}\text{O}$ -Na and (B)  $\delta^{18}\text{O}$ -Sr correlation graphs of type 1 dolomites from different sections: (●) Walhorn ( $r_{\text{Na}}: +0.88$ ,  $r_{\text{Sr}}: +0.38$ ); ( $\Delta$ ) Modave ( $r_{\text{Na}}: +0.78$ ,  $r_{\text{Sr}}: -0.82$ ); ( $\circ$ ) Saint Roch ( $r_{\text{Na}}: +0.67$ ,  $r_{\text{Sr}}: -0.23$ ); ( $\diamond$ ) Dolhain railway ( $r_{\text{Na}}: +0.69$ ,  $r_{\text{Sr}}: -0.92$ ); ( $\square$ ) Fonds de Forêt ( $r_{\text{Na}}: +0.80$ ,  $r_{\text{Sr}}: -0.91$ ); ( $\blacksquare$ ) Binsfeldhammer ( $r_{\text{Na}}: +0.10$ ,  $r_{\text{Sr}}: +0.31$ ).

texture is observed. However, the fine crystalline type 1A dolomites are generally the least  $^{18}\text{O}$  depleted ( $\delta^{18}\text{O} > -1\text{\textperthousand}$ ).

A  $\delta^{18}\text{O}$ -Na correlation is present in most profiles (Fig. 7A). The strongest correlation is observed within the dolomite belonging to the uppermost part of the dolomite sequence. No significant correlations between  $\delta^{18}\text{O}$  and other trace elements were observed. In some profiles, however, a negative  $\delta^{18}\text{O}$ -Sr correlation is present (Fig. 7B).

The type 2A saddle dolomites are somewhat more depleted in  $\delta^{13}\text{C}$  and  $\delta^{18}\text{O}$  (Fig. 6B and Table 3; respectively  $-1.35$  to  $+2.84\text{\textperthousand}$  and  $-20.45$  to  $-9.09\text{\textperthousand}$ ). The depleted  $\delta^{18}\text{O}$  values are in agreement with the interpretation that saddle dolomites precipi-

tate at higher temperatures ( $60$ – $150^\circ\text{C}$ , Radke & Mathis, 1980;  $90$ – $215^\circ\text{C}$ , Machel, 1987).

The type 2B saddle dolomites of the Aachen area have  $\delta^{13}\text{C}$  values of  $-0.01$  to  $+0.50\text{\textperthousand}$  and  $\delta^{18}\text{O}$  values of  $-6.90$  to  $-6.16\text{\textperthousand}$  (Fig. 6B and Table 3).

Some type 3 dolomite cements were analysed. They yield  $\delta^{13}\text{C}$  values of  $-1.74$  to  $+1.53\text{\textperthousand}$  and  $\delta^{18}\text{O}$  values of  $-11.00$  to  $-9.87\text{\textperthousand}$  (Fig. 6B and Table 3). However, these values are not necessarily representative for the whole spectrum of type 3 cement generations.

### Strontium isotopes

Sr isotope results of type 1 dolomites are distinctly more radiogenic ( $\sim 0.7088$  to  $0.7098$ ; Table 4) than values published for Lower Visean marine carbonates ( $\sim 0.7076$  to  $0.7078$ ; Burke *et al.*, 1982; Popp *et al.*, 1986; Douthit *et al.*, 1990). The Sr isotopic compositions vary within one sample from  $0.70882$  to  $0.70910$  (sample FF 9; Table 4). The  $^{87}\text{Sr}/^{86}\text{Sr}$  values of the type 2A saddle dolomites are even more radiogenic ( $\sim 0.7095$  to  $0.7113$ ; Table 4). For this limited set of data no apparent correlation exists between the Sr isotopes and the other measured parameters.

## DISCUSSION

Field and petrographic observations indicate that the main dolomitization event occurred early in the diagenetic history and that the dolomites are most likely to have originated from refluxing (hyper)saline brines or from seawater circulation near the mixing zone. The dolomites are nearly stoichiometric, yield low Na and Sr contents and display a wide spread in  $\delta^{18}\text{O}$  values. The latter shows that the various analysed minerals reflect a non-equilibrium assemblage.

Modern early diagenetic analogues, in contrast, are commonly enriched in  $^{18}\text{O}$  ( $\delta^{18}\text{O} = +2.5 \pm 2\text{\textperthousand}$ ; Land, 1985) and possess high Na and Sr contents (Land & Hoops, 1973). Furthermore, if the dolomites are marine derived they should have a near marine Early Visean strontium isotopic signature ( $\sim 0.7076$  to  $0.7078$ ). The Sr isotope results, however, display distinctly more radiogenic values ( $\sim 0.7088$  to  $0.7098$ ). This illustrates that there is an apparent conflict between the geological and geochemical evidence.

CL petrography allows the identification of various textures, which probably relate to recrystallization. The lack of CL zonation in most dolomites

**Table 4.**  $^{87}\text{Sr}/^{86}\text{Sr}$  ratios and  $\delta^{18}\text{O}$  and  $\delta^{13}\text{C}$  values ( $\text{\textperthousand}$ ) of some carefully selected samples.

Sample	Description	$^{87}\text{Sr}/^{86}\text{Sr}$ $2\sigma$	$\delta^{18}\text{O}$ $2\sigma$	$\delta^{13}\text{C}$ $2\sigma$
S8	type 1A, 20–50 $\mu\text{m}$ crystals; without visible recrystallization textures	0.709351 $\pm 0.000012$	-0.17 $\pm 0.01$	+3.61 $\pm 0.03$
FF9	type 1B, 100–150 $\mu\text{m}$ crystals; nearly without visible recrystallization textures	0.709290 $\pm 0.000011$	-1.82 $\pm 0.03$	+3.40 $\pm 0.03$
	with recrystallization textures (Fig. 4C); some intercrystalline type 3 dolomite cement	0.708819 $\pm 0.000015$	-1.56 $\pm 0.07$	+3.56 $\pm 0.03$
Sr9	type 1B, 120–150 $\mu\text{m}$ crystals; possibly vugs with type 3 dolomite cement; minor recrystallization (Fig. 4H)	0.709104 $\pm 0.000013$	-3.16 $\pm 0.07$	+0.98 $\pm 0.07$
	type 1B, 120–150 $\mu\text{m}$ crystals; blotchy recrystallization	0.709100 $\pm 0.000053$	-9.18 $\pm 0.05$	+1.32 $\pm 0.04$
S27	type 1B, 50–100 $\mu\text{m}$ crystals; minor blotchy recrystallization	0.708844 $\pm 0.000011$	-13.51 $\pm 0.05$	+3.38 $\pm 0.02$
		0.709005 $\pm 0.000010$	-13.73 $\pm 0.02$	+3.53 $\pm 0.02$
Ri5	type 1B, 250–300 $\mu\text{m}$ crystals; minor blotchy recrystallization	0.709796 $\pm 0.000012$	-19.15 $\pm 0.04$	+4.37 $\pm 0.05$
Sr17	type 2A dolomite, cementing anhydrite mould	0.709866 $\pm 0.000012$	-14.83 $\pm 0.07$	+0.02 $\pm 0.02$
		0.709775 $\pm 0.000011$		
Sr21	type 2A dolomite, cementing anhydrite mould	0.709530 $\pm 0.000008$	-14.99 $\pm 0.03$	+0.89 $\pm 0.03$
FF9	type 2A dolomite, cementing crinoid mould	0.711263 $\pm 0.000014$	-10.73 $\pm 0.09$	+0.40 $\pm 0.12$

may be a primary feature. However, possible CL zoning may also have been obscured by the homogenization effect of recrystallization. The CL textures with interspersed patches are clearly not primary. The fact that patches occur adjacent to cement-free pores points to a replacement (recrystallization) rather than to a large scale dissolution–cementation origin. Similar luminescence characteristics have been reported in the literature for early stage dolomites extensively modified (recrystallized) by fluids precipitating late stage dolomite (Kupecz & Land, 1991). The zoned arrangement of patches possibly relates to primary differences in composition or to the presence of fluid inclusions or other impurities in certain crystal zones, which therefore were preferred locations for recrystallization. The irregular (truncation) contacts within some dolomite crystals (Fig. 4C–E) may reflect either overgrowth of a late dolomite on an early dolomite or partial replacement (recrystallization). The latter interpretation is

favoured in the cases in which patches of late dolomite occur within the early dolomite. Furthermore, these truncated crystals are not systematically larger in size, a feature which would probably develop if the textures related to overgrowth.

Based on the various textures interpreted as the products of recrystallization, these early dolomites have been subject to different recrystallization episodes. By invoking multiple recrystallization of the dolomites, the apparent conflict between geological evidence and geochemical data can be reconciled.

Locally, relics/ghosts of zoned CL patterns probably after type 3 dolomite cements are observed (Fig. 4G) within a relative homogeneously dull brown/red luminescent dolomite matrix. This indicates that at least one recrystallization episode also affected type 3 dolomites and thus testifies to late recrystallization. As some of the dolomite patches within the early dolomites have luminescence characteristics similar to certain type 3 dolomite cements (Fig. 4H), it is

appropriate to assume that recrystallization episodes occurred due to contact with these fluids, channelled along fractures. Microfractures of this kind can be seen to cut dolomite crystals influenced by at least one earlier recrystallization episode.

Although the stoichiometric nature of the dolomites is interpreted here to be the result of (multiple) recrystallization, it cannot be excluded that the dolomites were initially stoichiometric.

The  $\delta^{13}\text{C}$  values of the type 1 dolomites (with or without visible recrystallization features) plot within the range of Lower Carboniferous marine carbonates. Consequently, the initial  $\delta^{13}\text{C}$  composition of these dolomites did not change drastically during recrystallization. This suggests that the fluids responsible for alteration of the precursor dolomites had a similar  $\delta^{13}\text{C}$  composition to Dinantian marine carbonates or were buffered by these carbonates.

The reported estimates for the  $\delta^{18}\text{O}$  composition of Lower Carboniferous marine limestones vary between  $-4.0$  and  $-1.0\text{\textperthousand}$  PDB (Brand, 1982; Meyers & Lohmann, 1985; Lohmann, 1987; Hudson & Anderson, 1989; Walkden & Williams, 1991). Since dolomites are enriched in  $\delta^{18}\text{O}$  by  $3 \pm 1\text{\textperthousand}$  compared with syngenetic calcite (Clayton *et al.*, 1968; Aharon *et al.*, 1977; McKenzie, 1981; Land, 1985), dolomites which precipitated in equilibrium with Early Carboniferous seawater should have a  $\delta^{18}\text{O}$  composition between  $+2$  and  $-1\text{\textperthousand}$ .

Only some of the finely crystalline type 1A dolomites have a  $\delta^{18}\text{O}$  composition that falls within this range. They predominantly occur in a high stratigraphical position, commonly have higher Na (Fig. 7A) and sometimes also higher Sr contents (Fig. 7B). They show little petrographical evidence for recrystallization. The higher clay and organic matter content in these strata, enveloping the dolomite crystals, suggests that these non-carbonate impurities cause a shielding effect, inhibiting large scale recrystallization of the type 1A dolomites. A similar 'shielding effect' has been invoked in the literature to explain, for example, abnormally high Sr contents in carbonates where the individual particles are surrounded by clays or organic matter (Kranz, 1973; Swennen & Viaene, 1981). A similar relation between Na, Sr and  $\delta^{18}\text{O}$  values has been documented by other authors. Middle Devonian dolomites interpreted by Fritz (1971) as having formed from highly saline,  $^{18}\text{O}$ -rich solutions have  $\delta^{18}\text{O}$  values of  $-4$  to  $-1\text{\textperthousand}$  and Na contents of about 200–700 ppm. 'Unaltered' Mississippian dolomites described by Smith & Dorobek (in press) contain  $\delta^{18}\text{O}$  values more positive

than  $-1.5\text{\textperthousand}$  and Na contents above 350 ppm. All the above dolomites typically were dolomudstones and cryptagalaminites, which most likely also possess higher contents of non-carbonate impurities.

The coarsely crystalline (type 1B) and many of the finely crystalline (type 1A) dolomites, however, are more depleted in  $^{18}\text{O}$  and are characterized by low trace element contents and rather high  $^{87}\text{Sr}/^{86}\text{Sr}$  values. Whether the coarse crystal sizes are the product of crystal enlargement is unclear. The modified geochemical nature of these dolomites could also be due to preferential and longer lasting fluid circulation within these generally more porous dolomites. Since the dolomites are early diagenetic (Lower Visean) this suggests a resetting of the geochemical composition:

- 1 within  $^{18}\text{O}$ -depleted fluids and/or at elevated temperatures;
- 2 within  $\text{Fe}^{2+}$ - and  $\text{Mn}^{2+}$ -poor fluids (since the distribution coefficients of these elements are larger than 1; Veizer, 1983); and
- 3 within fluids enriched in  $^{87}\text{Sr}/^{86}\text{Sr}$  (compared with Early Carboniferous seawater).

Recrystallization is documented to take place in various diagenetic realms, starting from near surface (McKenzie, 1981; Carballo *et al.*, 1987; Gregg & Shelton, 1990; Gregg *et al.*, 1992) to deeper burial conditions (Banner *et al.*, 1988; Cander *et al.*, 1988; Gregg & Shelton, 1990).

Whether early syndepositional neomorphism affected these dolomites is not inferrable, since relics of pre-neomorphosed dolomite generations have not been identified. However, since several karst horizons occur within the upper Palaeozoic strata close to the Brabant-Wales Massif (Paproth *et al.*, 1983a,b), significant amounts of meteoric water could have circulated through the dolomites since their formation. The dolomite characteristics in these areas are consistent with the results obtained by Smith & Dorobek (in press) for meteoric recrystallization, i.e. nearly stoichiometric and  $^{18}\text{O}$ - and trace element-depleted dolomites. The most depleted dolomites have  $\delta^{18}\text{O}$  values as light as  $-19\text{\textperthousand}$ . Such light values cannot be explained by meteoric recrystallization at a shallow depth.

Recrystallization due to interaction with solutions from which also late dolomites precipitate is sometimes invoked in the literature (Kupecz & Land, 1991; Amthor & Friedman, 1992; Montañez & Read, 1992b). The type 2A saddle dolomites have  $\delta^{18}\text{O}$  values ( $-20.54$  to  $-9.09\text{\textperthousand}$ ; Fig. 6B) which match those of the  $^{18}\text{O}$ -depleted type 1 dolomites (Fig. 6B).

These saddle dolomites are furthermore characterized by very low Fe and Mn contents (Table 2) and high  $^{87}\text{Sr}/^{86}\text{Sr}$  ratios (Table 4). Thus, although no apparent petrographic evidence for involvement of these saddle dolomite precipitating fluids can be given, recrystallization due to interaction with these fluids would result in the observed modifications of the type 1 dolomites.

Some of the type 1 dolomites have crystal domains with similar luminescence characteristics as nearby type 3 dolomite cements. It is therefore likely that some of the recrystallization processes relate to interaction with these fracture related fluids. Dolomites that recrystallize during this period will experience a shift in  $\delta^{18}\text{O}$  towards type 3 dolomite cement compositions ( $-11.00$  to  $-9.87\text{\textperthousand}$ ; Table 4). Recrystallization under these circumstances may lead to  $^{18}\text{O}$  depletion of yet unaltered or only slightly altered dolomites or even to  $^{18}\text{O}$  enrichment of previously altered and strongly depleted dolomites. Some of the dolomites with clear recrystallization textures related to interaction with type 3 dolomite solutions are in fact less  $^{18}\text{O}$  depleted than nearby seemingly unaltered dolomites.

Other mainly fracture related fluids that could have influenced the geochemistry of the dolomites are MVT mineralizing fluids. In the eastern part of the study area important MVT mineralizations occur (Dejonghe & Jans, 1983). Saddle dolomites (type 2B) that developed in association with these MVT mineralizations have  $\delta^{18}\text{O}$  compositions of  $-6.90$  to  $-6.16\text{\textperthousand}$ . Recrystallization that caused important negative shifts of the initial  $^{18}\text{O}$  signature of Lower Dinantian dolomites are not to be expected from these fluids; however, a slight shift in  $\delta^{18}\text{O}$  is possible and even highly depleted recrystallized dolomites may evolve towards less depleted values.

Of all these fluids, the type 2A saddle dolomite fluid has probably passed through the host dolomites in the most pervasive way, precipitating saddle dolomite in open pores and voids. All other fluids were rather channelled through the dolomites along fractures. Fluid infiltration distances from fracture surfaces into host rock are often considered to be relatively low (Frimmel, 1992). It is therefore likely that the major recrystallization episode relates to the formation of the type 2A saddle dolomites.

The presumed driving forces behind dolomite recrystallization cited in the literature are as follows.

**1** An increase in stability, i.e. lowering of the free energy. Poorly ordered and non-stoichiometric dolo-

mites have high free energies and are therefore prone to dissolution and/or neomorphic alteration by a process of dissolution–reprecipitation to form dolomite with ‘ideal’ stoichiometry and ordering (Katz & Matthews, 1977; Reeder, 1981; Gregg & Sibley, 1984; Sibley, 1990).

**2** A reduction of the surface energy, i.e. the process by which finely crystalline mosaics have the tendency to recrystallize to coarser crystals (Gregg & Sibley, 1984; Gregg & Shelton, 1990; Gregg *et al.*, 1992).

**3** A reduction of crystal defects (Sibley, 1990).

A remarkable feature in our dataset is the fact that the present day  $\delta^{18}\text{O}$  and  $^{87}\text{Sr}/^{86}\text{Sr}$  values display a wide range. This indicates that dolomite recrystallization did not reach equilibrium with a single unique condition.  $\delta^{18}\text{O}$  values within some crystals have been reset, whilst others seem to have been retained and were reset possibly later. This non-equilibrium status shows that despite the fact that the different dolomite crystals (on micro- and macro-scale) were subject to the same diagenetic fluids, they reacted differently. This suggests that dolomites are ‘highly reactive diagenetic bombs’ possessing variable ‘recrystallization potentials’. Even within one crystal different crystal domains seem to behave differently. The ‘recrystallization potential’ seems to differ from place to place and changes throughout the diagenetic history of the dolomites.

Transmission electron microscope studies of replacement dolomites and dolomite cements have revealed microstructural differences between dolomite types and demonstrated heterogeneous microstructures within individual crystals (Reeder, 1981; Freeman *et al.*, 1983; Barber *et al.*, 1985). Reeder (1981) documented regions of modulated and homogeneous microstructure in sedimentary dolomite crystals with intermediate compositions (excess of 1–3 mol%  $\text{CaCO}_3$ ), suggesting a mixture of stoichiometric and calcian regions. Reeder (1981) concluded that these microstructural differences reflect processes affecting the mineral following precipitation. The recrystallization potential is possibly comparable with the energy barrier which governs metamorphic recrystallization reactions (Vernon, 1976). Lowering of the activation energy is caused here by the fluid involved which acts as a catalyst. However, within dolomites it seems to be less predictable, possibly since non-equilibrium crystallization is involved (Reeder, 1981).

The recrystallization potential not only relates to the nature of the dolomite crystals but also to the

nature and transferability of diagenetic fluids. The dolomite mineralogy (stoichiometry, ordering state, presence of non-equilibrium crystal domains), crystal size, presence of intracrystalline impurities, fluid inclusions, etc., relate to the original dolomitization environment and/or dolomitization process and are likely to determine whether a dolomite crystal is prone to recrystallize. In order to alter the dolomites effectively the recrystallization process relies on the presence of a fluid film between reactant and recrystallization product. The reactivity of the fluids depends on the respective nature of the fluid and the initial dolomite crystals. Highly permeable lithologies obviously favour the presence of diagenetic fluids. Thus, the potential of dolomites to be affected by diagenetic fluids also depends on the porous or non-porous character of the dolomite rocks (i.e. on the transferability of diagenetic fluids). Furthermore, clays and/or organic components may cause a 'shielding' effect, depending on how the non-carbonate minerals are distributed. A resetting of the recrystallization potential takes place whenever a dolomite crystal re-equilibrates with a fluid.

Thus, the recrystallization of dolomite is a multiple-step process which does not necessarily lead to a complete homogenization of the petrographic or chemical characteristics of the dolomites.

## CONCLUSIONS

Field evidence and petrographic and geochemical data complement the study of the Lower Dinantian dolomites in south and south-eastern Belgium. The following major conclusions can be drawn from this research.

**1** Based on field observations, dolomitization of the Tournaesian and Lower Visean shallow subtidal limestones is of Early Visean age. Adjacent to the Brabant-Wales palaeo-high, a karst horizon marks the contact between the dolomite and the overlying Lower Visean crinoidal and oolitic limestones. In the shelf interior (Vesdre-Ourthe area) an important evaporitic collapse breccia is present between the dolomites and Lower Visean peritidal limestones.

**2** Reflux dolomitization by (hyper)saline brines and/or dolomitization by seawater in relation to circulation near the mixing zone during a period of sea level lowstand are viable models to explain the development of the massive Lower Dinantian dolomites.

**3** Field data and relationships should be taken into account as a guide to the origin of ancient dolomites.

**4** Alteration of the original trace element and isotopic signature of the investigated dolomites relates to recrystallization. The large range in  $\delta^{18}\text{O}$  values proves that isotopic resetting was a complex multi-step process. The different possibly interactive episodes are recrystallization (i) by meteoric solutions, (ii) by solutions which caused type 2A saddle dolomite formation, (iii) by MVT-type related solutions, and (iv) by solutions channelled through fractures giving rise to type 3 dolomites. Whether this list of episodes is complete for the envisaged dolomite is unclear.

**5** Different recrystallization textures have been identified by the use of CL and fluorescence microscopy. However, dolomites with no petrographic indications of recrystallization may also possess an altered geochemical signature, illustrating that not all recrystallization phenomena are recognized with the presently available petrographical techniques.

**6**  $\delta^{18}\text{O}$  resetting due to recrystallization is less obvious in finely crystalline dolomites where the individual crystals are shielded by organic matter and/or clays. The Na content of these samples is also higher. This lithology therefore gives the best estimate of the initial isotope and least altered trace element composition.

**7** Dolomites can be considered as 'diagenetic time-bombs'. The different dolomite crystals which make up a dolomite rock seem to possess different recrystallization potentials. Even within individual crystals this potential does not seem to be homogeneous. This behaviour explains why the  $\delta^{18}\text{O}$  values of dolomite samples from one locality or even from one hand specimen cover a wide range.

The 'dolomite problem' thus not only relates to the process of dolomite formation but should be extended to its diagenetic reactivity.

## ACKNOWLEDGMENTS

Sr isotopic analyses were carried out at the Belgian Centre for Geochronology with considerable support from D. Weis and C. Gilson. Earlier drafts of this paper benefited from the critical review and suggestions of Ph. Muchez, J.A.D. Dickson, J.M. Gregg, M.E. Tucker and S.D. Burley. Thin sections and most of the AAS analyses were provided through the efforts of C. Moldenaers, H. Nijs and D. Coetemans. This research was partly supported by a grant from the National Fund of Scientific research of Belgium (project No. 9.00.47.89: SEM-research and project No. 2.0062.91N: XRD-research).

## REFERENCES

- AHARON, P., KOLODNY, Y. & SASS, E. (1977) Recent hot brine dolomitization in the "solar lake", Gulf of Elat, Isotopic, Chemical, and Mineralogical study. *J. Geol.*, **85**, 27–48.
- AMTHOR, J.E. & FRIEDMAN, G.M. (1992) Early- to late-diagenetic dolomitization of platform carbonates: Lower Ordovician Ellenburger group, Permian basin, West Texas. *J. sedim. Petrol.*, **62**, 131–144.
- BANNER, J.L., HANSON, G.N. & MEYERS, W.J. (1988) Water-rock interaction history of regionally extensive dolomites of the Burlington-Keokuk Formation (Mississippian): isotopic evidence. In: *Sedimentology and Geochemistry of Dolostones* (Ed. by V. Shukla and P. A. Baker), *Spec. Publ. Soc. econ. Paleont. Miner.*, **43**, 97–113.
- BARBER, D.J., REEDER, R.J. & SMITH, D.J. (1985) A TEM microstructural study of dolomite with curved faces (saddle dolomite). *Contrib. Mineral. Petrol.*, **91**, 82–92.
- BLESS, M., BOUCKAERT, J., CONIL, R. et al. (1980) Pre-Permian sedimentation in NW Europe. *Sediment. Geol.*, **27**, 1–81.
- BOONEN, P. & KASIG, W. (1979) Das Dinantium zwischen Aachen und Lüttich. *Z. dt. geol. Ges.*, **130**, 123–143.
- BRAND, U. (1982) The oxygen and carbon isotope composition of Carboniferous fossil components: sea-water effects. *Sedimentology*, **29**, 139–147.
- BURKE, W.H., DENISON, R.E., HETHERINGTON, E.A., KOEPNICK, R.B., NELSON, H.F. & OTTO, J.B. (1982) Variation in  $^{87}\text{Sr}/^{86}\text{Sr}$  throughout Phanerozoic time. *Geology*, **10**, 516–519.
- CANDER, H.S., KAUFMAN, J., DANIELS, L.D. & MEYERS, W.J. (1988) Regional dolomitization of shelf carbonates in the Burlington-Keokuk formation, Illinois and Missouri: Constraints from cathodoluminescent zonal stratigraphy. In: *Sedimentology and Geochemistry of Dolostones* (Ed. by V. Shukla and P. A. Baker), *Spec. Publ. Soc. econ. Paleont. Miner.*, **43**, 97–113.
- CARBALLO, J.D., LAND, L.S. & MISER, D.E. (1987) Holocene dolomitization of supratidal sediments by active tidal pumping, Sugoarloaf Key, Florida. *J. sedim. Petrol.*, **57**, 153–165.
- CLAYTON, R.N., JONES, B.F. & BERNER, R.A. (1968) Isotope studies of dolomite formation under sedimentary conditions. *Geochim. Cosmochim. Acta*, **32**, 415–432.
- CRAIG, H. (1957) Isotopic standards for carbon and oxygen correction factors for mass spectrometric analysis of carbon dioxide. *Geochim. Cosmochim. Acta*, **12**, 133–149.
- DEJONGHE, L. & JANS, D. (1983) Les gisements plombozincifères de l'Est de la Belgique. *Chron. Rech. Min.*, **470**, 3–24.
- DOUTHIT, T.L., HANSON, G.N. & MEYERS, W.J. (1990) Structure in the secular variation of seawater  $^{87}\text{Sr}/^{86}\text{Sr}$  for the Ivorian/Chadian (Osagean, Lower Carboniferous). *Bull. Am. Ass. petrol. Geol.*, **74**, 644.
- DRAVIS, J.J. & YUREWICZ, D.A. (1985) Enhanced carbonate petrography using fluorescence microscopy. *J. sedim. Petrol.*, **55**, 795–804.
- FREEMAN, L.A., BARBER, D.J., O'KEEFE, M.A. & SMITH, D.J. (1983) High resolution studies of defects in natural dolomites. In: *Proc. 7th Int. Conf. High Voltage Elecron Microsc.*, pp. 377–380. Lawrence Berkeley Laboratory, University of California, Berkeley.
- FRIMMEL, H.E. (1992) Isotopic fronts in hydrothermally mineralized carbonate rocks. *Mineral. Deposita*, **27**, 257–267.
- FRITZ, P. (1971) Geochemical characteristics of dolomites and the  $^{18}\text{O}$  content of Middle Devonian oceans. *Earth planet. Sci. Lett.*, **11**, 277–282.
- GAO, G. (1990) Geochemical and isotopic constraints on the diagenetic history of a massive stratal, late Cambrian (Royer) dolomite, Lower Arbuckle Group, Slick Hills, SW Oklahoma, USA. *Geochim. Cosmochim. Acta*, **54**, 1979–1989.
- GAO, G. & LAND, L.S. (1991) Early Ordovician Cool Creek dolomite, Middle Arbuckle Group, Slick Hills, SW Oklahoma, USA. Origin and Modification. *J. sedim. Petrol.*, **61**, 161–173.
- GIVEN, R.K. & WILKINSON, B.H. (1987) Dolomite abundance and stratigraphic age: constraints on rates and mechanisms of Phanerozoic dolostone formation. *J. sedim. Petrol.*, **57**, 1068–1078.
- GREGG, J.M., HOWARD, S.A. & MAZZULLO, S.J. (1992) Early diagenetic recrystallization of Holocene (<3000 years old) peritidal dolomites, Ambergris Cay, Belize. *Sedimentology*, **39**, 143–160.
- GREGG, J.M. & SHELTON, K.L. (1990) Dolomitization and dolomite neomorphism in the back reef facies of the Bonneterre and Davis Formations (Cambrian), southeastern Missouri. *J. sedim. Petrol.*, **60**, 549–562.
- GREGG, J.M. & SIBLEY, D.F. (1984) Epigenetic dolomitization and the origin of xenotopic dolomite texture. *J. sedim. Petrol.*, **54**, 908–931.
- HARLAND, W.B., ARMSTRONG, R.L., COX, A.V., CRAIG, L. E., SMITH A.G. & SMITH, D.G. (1989) In: *A Geological Time Scale 1989*, pp. 42–46. Cambridge University Press.
- HUDSON, J.D. & ANDERSON, T.F. (1989) Ocean temperatures and isotopic compositions through time. *Trans. R. Soc. Edin.*, **80**, 183–192.
- KASIG, W. (1980) Dinantian carbonates in the Aachen region, Federal Republic of Germany. *Mededeling Rijks. Geol. dienst.*, **32**, 44–52.
- KATZ, A. & MATTHEWS, A. (1977) The dolomitization of  $\text{CaCO}_3$ : an experimental study at 252–295°C. *Geochim. Cosmochim. Acta*, **41**, 297–308.
- KRANZ, J.R. (1973) Die Strontium-Verteilung in den Arlbergschichten (Obere Ladin) des Kloster Tales (Voralberg). Nördliche Kalkalpen. *N. Jb. Geol. Paläont. Mh.*, **3**, 170–187.
- KUPECZ, J.A. & LAND, L.S. (1991) Late-stage dolomitization of the Lower Ordovician Ellenburger Group, West Texas. *J. sedim. Petrol.*, **61**, 551–574.
- LAND, L.S. (1980) The isotopic and trace element geochemistry of dolomite: the state of the art. In: *Concepts and Models of Dolomitization* (Ed. by D. G. Zenger, J. B. Dunham and R. L. Ethington), *Spec. Publ. Soc. econ. Paleont. Miner.*, **28**, 87–110.
- LAND, L.S. (1985) The origin of massive dolomite. *J. Geol. Education*, **33**, 112–125.
- LAND, L.S. & HOOPS, G.K. (1973) Sodium in carbonate sediments and rocks: a possible index to the salinity of diagenetic solutions. *J. sedim. Petrol.*, **43**, 614–617.

- LOHMANN, K.C. (1987) Geochemical patterns of meteoric diagenetic systems and their application to studies of paleokarst. In: *Paleokarst* (Ed. by N. P. James and P. W. Choquette), pp. 58–80. Springer-Verlag, Berlin.
- LUMSDEN, D.N. (1979) Discrepancy between thin-section and X-ray estimates of dolomite in limestone. *J. sedim. Petrol.*, **49**, 429–436.
- MACHEL, H.G. (1987) Saddle dolomite as a by-product of chemical compaction and thermochemical sulphate reduction. *Geology*, **15**, 936–940.
- MALIVA, R.G. (1987) Quartz geodes: early diagenetic silicified anhydrite nodules related to dolomitization. *J. sedim. Petrol.*, **57**, 1054–1059.
- MCKENZIE, J.A. (1981) Holocene dolomitization of calcium carbonate sediments from the coastal sabkhas of Abu Dhabi, U.A.E.: a stable isotope study. *J. Geol.*, **89**, 185–198.
- MEYERS, W.J. & LOHMANN, K.C. (1985) Isotope geochemistry of regionally extensive calcite cement zones and marine components in Mississippian limestones, New Mexico. In: *Carbonate Cements* (Ed. By N. Schneidermann and P. M. Harris), *Spec. Publ. Soc. econ. Paleont. Miner.*, **36**, 223–239.
- MONTAÑEZ, I.P. & READ, J.F. (1992a) Eustatic control on early dolomitization of cyclic peritidal carbonates: Evidence from the Early Ordovician Upper Knox Group, Appalachians. *Bull. geol. Soc. Am.*, **104**, 872–886.
- MONTAÑEZ, I.P. & READ, J.F. (1992b) Fluid-rock interaction history during stabilization of early dolomites. Upper Knox Group (Lower Ordovician), U.S. Appalachians. *J. sedim. Petrol.*, **62**, 753–778.
- MUCHEZ, P. (1988) *Sedimentologische, diagenetische en geochemische studie van de Dinantiaan strata ten noorden van het Brabant Massief (Bekken van de Kempen)*. PhD Thesis, Katholieke Universiteit Leuven.
- ONCKEN, O. (1984) Zusammenhänge in der Strukturgeneese des Rheinischen Schiefergebirges. *Geol. Rdsch.*, **73**, 619–649.
- PAPROTH, E., CONIL, R., BLESS, M.J.M., et al. (1983a) Bio- and lithostratigraphic subdivisions of the Dinantian in Belgium. A review. *Ann. Soc. géol. Belg.*, **106**, 1–82.
- PAPROTH, E., DUSAR, M., BLESS, M.J.M., et al. (1983b) Bio- and lithostratigraphic subdivisions of the Silesian in Belgium. A review. *Ann. Soc. géol. Belg.*, **106**, 241–283.
- PEETERS, C., MUCHEZ, Ph. & VIAENE, W. (1992b) Paleogeographic and climatic evolution of the Moliniacian (lower Visean) in southeastern Belgium. *Geol. Mijnb.*, **71**, 39–50.
- PEETERS, C., SWENNEN, R., NIELSEN, P. & MUCHEZ, Ph. (1992a) Sedimentology and diagenesis of the visean carbonates in the Vesdre area (Verviers synclinorium, E-Belgium). *Zbl. Geol. Paläont.*, **teil 1**, H.5, 519–547.
- PIREL, H. (1970) L'influence d'un karst sous-jacent sur la sédimentation calcaire et l'intérêt de l'étude des paléokarsts. *Ann. Soc. géol. Belg.*, **93**, 247–254.
- POPP, B.N., PODOSEK, F.A., BRANNON, J.C., ANDERSON, T.F. & PIER, J. (1986)  $^{87}\text{Sr}/^{86}\text{Sr}$  ratios in Perm-Carboniferous sea water from the analyses of well-preserved brachiopod shells. *Geochim. Cosmochim. Acta*, **50**, 1321–1328.
- RADKE, B.M. & MATHIS, R.L. (1980) On the formation and occurrence of saddle dolomite. *J. sedim. Petrol.*, **50**, 1149–1168.
- REEDER, R.J. (1981) Electron optical investigations of sedimentary dolomites. *Contrib. Mineral. Petrol.*, **76**, 148–157.
- ROSS, C.A. & ROSS, J.R.P. (1987) Late Palaeozoic sea-levels and depositional sequences. *Spec. Publ. Cushman Foundation of Foram. Res.*, **24**, 137–149.
- SIBLEY, D.F. (1990) Unstable to stable transformations during dolomitization. *J. Geol.*, **98**, 739–748.
- SIBLEY, D.F. & GREGG, J.M. (1987) Classification of dolomite rock textures. *J. sedim. Petrol.*, **57**, 967–975.
- SMITH, T.M. & DOROBEC, S.L. (in press) Meteoric recrystallization of early-formed dolomite: Mississippian Mission Canyon Formation, Montana. *Bull. geol. Soc. Am.*
- SPERBER, C.M., WILKINSON, B.H. & PEACOR, D.R. (1984) Rock composition, dolomite stoichiometry, and rock/water reactions in dolomitic carbonate rocks. *J. Geol.*, **92**, 609–622.
- SWENNEN, R. (1986) Lithogeochemistry of Dinantian carbonates in the Vesdre basin (Verviers Synclinorium: E-Belgium) and its relation to paleogeography, lithology, diagenesis and Pb-Zn mineralisations. In: *Academica Analecta, Academy of Science, Klasse der Wetenschappen*, **48**, 67–108. Paleis der Academiën, Brussels, Brepols Publishers.
- SWENNEN, R., PEETERS, C., MUCHEZ, Ph., MAES, K. & VIAENE, W. (1988) Sedimentological and diagenetic evolution of dinantian carbonates (dolomitization, evaporite solution collapse breccias, paleosols and palisade calcites). In: *Exc. Guidebook – 9th European Meeting of the IAS* (Ed. by A. Herbosch), pp. 77–97. Ministry for Economic Affairs, Belg. Geol. Soc., Brussels.
- SWENNEN, R. & VIAENE, W. (1981) Lithogeochemistry of some carbonate sections of the Dinantian in the Vesdre region (Belgium). *Bull. Soc. géol. Belg.*, **90**, 65–80.
- SWENNEN, R. & VIAENE, W. (1986) Occurrence of pseudomorphosed anhydrite nodules in the Lower Visean (Lower Moliniacian of the Verviers synclinorium, E-Belgium). *Bull. Soc. géol. Belg.*, **95**, 89–99.
- SWENNEN, R. & VIAENE, W. (1990) Lithogeochemical patterns around Pb-Zn mineralisations in Dinantian carbonate rocks of (eastern) Belgium. *Miner. Deposita*, **25**, 251–261.
- SWENNEN, R., VIAENE, W., BOUCKAERT, J., SIMAKOV, K.V. & VAN OYEN, P. (1986) Lithogeochemistry of Upper Famennian-Tournaisian strata in the Omolom area (WE-USSR) and its implications. *Ann. Soc. géol. Belg.*, **109**, 249–261.
- SWENNEN, R., VIAENE, W. & CORNELISSEN, C. (1990) Petrography and geochemistry of the Bell Roche breccia (Lower Visean, Belgium): evidence for brecciation by evaporite dissolution. *Sedimentology*, **37**, 859–878.
- SWENNEN, R., VIAENE, W., JACOBS, L. & VAN ORSMAAL, J. (1981) Occurrence of calcite pseudomorphs after gypsum in the Lower Carboniferous of the Vesdre region (Belgium). *Bull. Soc. géol. Belg.*, **90**, 231–247.
- VEIZER, J. (1983) Chemical diagenesis of carbonates: theory and application of trace element technique. In: *Stable Isotopes in Sedimentary Petrology* (Ed. by M. A. Arthur et al.), *Soc. econ. Paleont. Miner. Short Course*, **10**, 3-1–3-100.
- VERNON, R.H. (1976) *Metamorphic Processes: Reactions and Microstructure Development*. Thomas Murby, London.

- VIEL, P. (1984) *Contribution à l'étude Bio- et Lithostratigraphique de la limite Tournaisien-Viséen dans le bord oriental du synclinal de Namur*. Lic. thesis, Université de Liège.
- VOGEL, K., MUCHEZ, Ph. & VIAENE, W. (1991) Collapse breccias and sedimentary conglomerates in the Lower Visean of the Vesdre area (E-Belgium). *Ann. Soc. géol. Belg.*, **113**, 359–371.
- WALKDEN, G.M. & WILLIAMS, D.O. (1991) The diagenesis of the late Dinantian Derbyshire–East Midland carbonate shelf, central England. *Sedimentology*, **38**, 643–670.

(Manuscript received 11 August 1992; revision accepted 14 December 1993)